Supplementary Material For

Modular Pathway Engineering of Diterpenoid Synthases and the Mevalonic Acid Pathway for Miltiradiene Production in Yeast

Yongjin J. Zhou,[#, †, ‡] Wei Gao,[$, §, ‡] Qixian Rong,[$] Guojie Jin,[#, †] Huiying Chu,[&] Wujun Liu,[#] Wei Yang,[#] Zhiwei Zhu,[#, †] Guohui Li,[&] Guofeng Zhu,[¶] Luqi Huang,[*, $] and Zongbao K. Zhao[*, #]

Division of Biotechnology, Dalian Institute of Chemical Physics, CAS, Dalian 116023, PR China

$ Institute of Chinese Materia Medica, CACMS, Beijing 100700, China

& State Key Laboratory of Molecular Reaction Dynamics, Dalian Institute of Chemical Physics, CAS, Dalian 116023, PR China

§ School of Traditional Chinese Medicine, Capital Medical University, Beijing 100069, China

¶ Institute of Pathogen Biology, CAMS, Beijing 100730, China

† Graduate University of Chinese Academy of Sciences, Beijing 100049, PR China

‡ These authors contributed equally

Correspondence should be addressed to L.Q.H. (huangluqi@263.net) or Z.K.Z

(zhaozb@dicp.ac.cn).

Table S1. *S. cerevisiae* strains used in this study.

Strains	**Genotype or characteristic**	**Resource**
BY4741	*MATa; his3Δ1; leu2Δ0; met15Δ0; ura3Δ0*	ATCC
BY4742	*MATα; his3Δ1; leu2Δ0; lys2Δ0; ura3Δ0*	ATCC
YJ1	BY4741/pYX212-(*SmCPS-SmKSL*)	This study
YJ2	BY4741/pYX212-(*SmKSL-SmCPS*)	This study
YJ5	BY4741/pYX212-*SmCPS*+*SmKSL*	This study
YJ6	BY4741/pYX212-*ERG20*+*SmCPS*+*SmKSL*	This study
YJ7	BY4741/pYX212-*BTS1*+*SmCPS*+*SmKSL*	This study
YJ8	BY4741/pYX212-*BTS1*+*ERG20*+*SmCPS*+*SmKSL*	This study
YJ9	BY4741/pYX212-(*ERG20-BTS1*)+*SmCPS*+*SmKSL*	This study
YJ10	BY4741/pYX212-(*BTS1-ERG20*)+*SmCPS*+*SmKSL*	This study
YJ13	BY4741/pYX212-(*BTS1-ERG20*)+(*SmCPS-SmKSL*)	This study
YJ14	BY4741/pYX212-(*BTS1-ERG20*)+(*SmKSL-SmCPS*)	This study
YJ16	BY4741/pYX212-*SmCPS*+*SmKSL*/p424-*HMG1*	This study
YJ17	BY4741/pYX212-*SmCPS*+*SmKSL*/p424-*tHMG1*	This study
YJ19	BY4741/pYX212-(*BTS1-ERG20*)+ *SmCPS*+*SmKSL*/p424-*HMG1*	This study
YJ20	BY4741/pYX212-(*BTS1-ERG20*)+ *SmCPS*+*SmKSL*/p424-*tHMG1*	This study
YJ21	BY4741/δ-*tHMG1*-(*BTS1-ERG20*)+*SmCPS*+*SmKSL*	This study
YJ24	BY4741/*LEU2*/*MET15*/pYX212-(*BTS1-ERG20*)+*SmCPS*+*SmKSL*/p424-*tHMG1*	This study
YJ25	BY4741/*LEU2*/pYX212-(*BTS1-ERG20*)+*SmCPS*+*SmKSL*/p424-*tHMG1*	This study
YJ26	BY4741/pYX212-(*BTS1-ERG20*)+(*SmKSL-SmCPS*)/p424-*tHMG1*	This study
YJ27	BY4741/*LEU2*/pYX212-(*BTS1-ERG20*)+(*SmKSL-SmCPS*)/p424-*tHMG1*	This study
YJ28	BY4741/*LEU2*/*MET15*/pYX212-(*BTS1-ERG20*)+(*SmKSL-SmCPS*)/p424-*tHMG1*	This study
YJ2X	YJ27 mating with BY4742	This study

Table S2. Primers used for part cloning and module construction. The primer names were expressed in a format of 'part name-F' and 'part name-R', and the number in the brackets represent the strain number showed in Fig. 2c. For example, "TPIp(5)-F" stands for the forward primer to amplify TPI promoter, which used for the pathway construction of strain YJ5; "FBA1t (6)-R" represents the reverse primer for FBA1 terminator amplification in strain YJ6 construction.

Name	Sequence (5'-3')
Primers for episomal miltiradiene pathways construction	
TP1p(1,2,5-10)-F	GAATTGGGGATCTACGTATGGTC
TPIp(1,2,5)-R	CTATATCAATTAATTTGAATTAACAGTTTATGTATGTGTTTTTTG
FBA1t(1,2,5)-F	CAAAAAACACATACATAAACTGTTAATTCAAATTAATTGATATAG
FBA1t(1,2,5-10)-R	GAGTAGAAACATTTTGAAGCTATAGTAAGCTACTATGAAAGACTTTAC
TPIp(6,8,9)-R	CTATATCAATTAATTTGAATTAACAGTTTATGTATGTGTTTTTTG
ERG20(6,8,9)-F	CAAAAAACACATACATAAACTAAAAATGGCTTCAGAAAAAGAAATTAG
ERG20(6,8,10)-R	CTATATCAATTAATTTGAATTAACCTATTTGCTTCTCTTGTAAAC
FBA1t(6,8,10)-F	GTTTACAAGAGAAGCAAATAGGTTAATTCAAATTAATTGATATAG
TPIp(7,8,10)-R	CAGCTCATCTATCTTGGCCTCCATTTTTAGTTTATGTATGTGTTTTTTG
BTS1(7,8,10)-F	CAAAAAACACATACATAAACTAAAAATGGAGGCCAAGATAGATGAGCTG
BTS1(7,8,9)-R	CTATATCAATTAATTTGAATTAACTCACAATTCGGATAAGTGG
FBA1t(7,8,9)-F	GACCACTTATCCGAATTGTGAGTTAATTCAAATTAATTGATATAG
ERG20(9)-R	CTCATCTATCTTGGCCTCCATAGAACCACCACCTTTGCTTCTCTTGTAAACTTTG
BTS1(9)-F	CAAAGTTTACAAGAGAAGCAAAGGTGGTGGTTCTATGGAGGCCAAGATAGATGAG
BTS1(10)-R	CTGAAGCCATAGAACCACCACCCAATTCGGATAAGTGGTCTATTATATATAAC
ERG20(10)-F	GACCACTTATCCGAATTGGGTGGTGGTTCTATGGCTTCAGAAAAAGAAATTAG
TEF1p(5-10)-F	GTAAAGTCTTTCATAGTAGCTTACTATAGCTTCAAAATGTTTCTACTC
TEF1p(5-10)-R	GATTGTAGAGGATAAGGAGGCCATTTTGTAATTAAAACTTAGATTAGATTG
SmCPS(5-10)-F	CAATCTAATCTAAGTTTTAATTACAAAATGGCCTCCTTATCCTCTACAATC
SmCPS(5-10)-R	CATTAAAGTAACTTAAGGAGTTAAATTCACGCGACTGGCTCGAAAAGCAC
TDH2t(5-10)-F	GCTTTTCGAGCCAGTCGCGTGAATTTAACTCCTTAAGTTACTTTAATG
TDH2t(5-10)-R	CAGTATTGATAATGATAAACTCGAGCGAAAAGCCAATTAGTGTGATAC
TDH3p(5-10)-F	GTATCACACTAATTGGCTTTTCGCTCGAGTTTATCATTATCAATACTG
TDH3p(5-10)-R	CCGGGTTGAAGGCGAGCGACATTTTGTTTGTTCTAGATCCGTCGAAACTAAG
SmKSL(5-10)-F	CTTAGTTTCGACGGATCTAGAACAAACAAAATGTCGCTCGCCTTCAACCCGG
SmKSL(5-10)-R	GACGCGTAAGCTTGTGGGCCCTATCATTTCCCTCTCACATTATTAGCTAC
pYX212t(5-10)-F	GTAGCTAATAATGTGAGAGGGAAATGATAGGGCCCACAAGCTTACGCGTC
pYX212t(5-10)-R	TGCCGTAAACCACTAAATCGGAACC

Supplementary Table 2 (continued.)

Name	Sequence
SmCPS(1,13)-R	GGTTGAAGGCGAGCGACATAGAACCACCACCCGCGACTGGCTCGAAAAGC
SmKSL(1,13)-F	GCTTTTCGAGCCAGTCGCGGGTGGTGGTTCTATGTCGCTCGCCTTCAACC
TEF1p(2,14)-R	GGTTGAAGGCGAGCGACATTTTGTAATTAAAACTTAGATTAG
SmKSL(2,14)-F	CTAATCTAAGTTTTAATTACAAAATGTCGCTCGCCTTCAACC
SmKSL(2,14)-R	GTAGAGGATAAGGAGGCCATAGAACCACCACCTTTCCCTCTCACATTATTAGC
SmKSL(2,14)-F	GCTAATAATGTGAGAGGGAAAGGTGGTGGTTCTATGGCCTCCTTATCCTCTAC
SmKSL(2,14)-R	GACGCGTAAGCTTGTGGGCCCTATCACGCGACTGGCTCG
pYX212t(2,14)-F	CGAGCCAGTCGCGTGATAGGGCCCACAAGCTTACGCGTC
HIS3-F	TGTCGGGGCTGGCTTAACTATG
HIS3-R	ACAAAAATTTAACGCGAATTTTAAC
P424HMG1-F	CAGAACTTAGTTTCGACGGATTCTAGAACTAGTAAAAATGCCGCCGCTATTCAAGGGAC
P424tHMG1-F	CAGAACTTAGTTTCGACGGATTCTAGAACTAGTAAAAATGGCTGCAGACCAATTGGTG
P424HMG1-R	GTGAATGTAAGCGTGACATAACTAATTACATGATTAGGATTTAATGCAGGTGAC
Primers for intergration miltiradiene pathways construction	
Ty1(Int)-F	GGAATAAAAATCCACTATCGTCTATCAAC
Ty1(Int)-R	GCTCTTAAAACGGGAATTTCATTGATCCTATTACATTATC
HIS3(Int)-F	GATAATGTAATAGGATCAATGAAATTCCCGTTTTAAGAG
HIS3(Int)-R	GATGTTATAATATCTGTGCGTGCATAGATCCGTCGAGTTCAAG
PGK1p(Int)-F	CTTGAACTCGACGGATCTATGCACGCACAGATATTATAACATC
PGK1p(Int)-R	CCTTGAATAGCGGCGGCATTTTGTTATATTTGTTGTAAAAAGTAG
tHMG1(Int)-F	CTACTTTTTACAACAAATATAACAAAATGGCTGCAGACCAATTGGTG
tHMG1(Int)-R	GTGACATAACTAATTACATGATTTAGGATTTAATGCAGGTGAC
Cyc1t(Int)-F	GTCACCTGCATTAAATCCTAAATCATGTAATTAGTTATGTCAC
Cyc1t(Int)-R	GACCATACGTAGATCCCCAATTCCATTAATGCAGGGCCGCAGC
TPIp(Int)-F	GCTGCGGCCCTGCATTAATGGAATTGGGGATCTACGTATGGTC
TPIp(Int)-R	CAGCTCATCTATCTTGGCCTCCATTTTTAGTTTATGTATGTGTTTTTTG
BTS1(Int)-F	CAAAAAACACATACATAAACTAAAAATGGAGGCCAAGATAGATGAGCTG
BTS1(Int)-R	CTGAAGCCATAGAACCACCACCCAATTCGGATAAGTGGTCTATTATATATAAC
FBA1t(Int)-F	GTTTACAAGAGAAGCAAATAGGTTAATTCAAATTAATTGATATAG
FBA1t(Int)-R	GAGTAGAAACATTTTGAAGCTATAGTAAGCTACTATGAAAGACTTTAC
TEF1p(Int))-F	GTAAAGTCTTTCATAGTAGCTTACTATAGCTTCAAAATGTTTCTACTC
TEF1p(Int))-R	GATTGTAGAGGATAAGGAGGCCATTTTGTAATTAAAACTTAGATTAGATTG
SmCPS(Int)-F	CAATCTAATCTAAGTTTTAATTACAAAATGGCCTCCTTATCCTCTACAATC
SmCPS(Int)-R	CATTAAAGTAACTTAAGGAGTTAAATTCACGCGACTGGCTCGAAAAGCAC
TDH2t(Int)-F	GCTTTTCGAGCCAGTCGCGTGAATTTAACTCCTTAAGTTACTTTAATG
TDH2t(Int)-R	CAGTATTGATAATGATAAACTCGAGCGAAAAGCCAATTAGTGTGATAC
TDH3p(Int)-F	GTATCACACTAATTGGCTTTTCGCTCGAGTTTATCATTATCAATACTG
TDH3p(Int)-R	CCGGGTTGAAGGCGAGCGACATTTTGTTTGTTCTAGATCCGTCGAAACTAAG

Supplementary Table 2 (continued)

Name	Sequence
SmKSL(Int)-F	CTTAGTTTCGACGGATCTAGAACAAACAAAATGTCGCTCGCCTTCAACCCGG
SmKSL(Int)-R	GACGCGTAAGCTTGTGGGCCCTATCATTTCCCTCTCACATTATTAGCTAC
pYX212t(Int)-F	GTAGCTAATAATGTGAGAGGGAAATGATAGGGCCCACAAGCTTACGCGTC
pYX212t(Int)-R	TGCCGTAAACCACTAAATCGGAACC
URA3(Int)-F	GTAGCTAATAATGTGAGAGGGAAATGATAGGGCCCACAAGCTTACGCGTC
URA3(Int)-R	CTCATTCCGTTTTATATGTTTGGGTGTTGGCGGGTGTCG
Ty2(Int)-F	CGACACCCGCCAACACCCAAACATATAAAACGGAATGAG
Ty2(Int)-R	GTGGGTAATTAGATAATTGTTGGGATTC
Primers for intergration miltiradiene pathway verification	
V-F1	CAAAATGGCTGCAGACCAATTGGTG
V-R1	TTCGGATAAGTGGTCTATTATATATAAC
V-F2	AGGTTAATTCAAATTAATTGATATAG
V-R2	TTGTTCTAGATCCGTCGAAACTAAG
Primers for auxotrophic marker complementation	
LEU2-F	CTTCATTATTACAGCCCTCTTGACCTCTAATCATGAATGTACTGTGGGAATAC
LEU2-R	GAGGTCGACTACGTCGTTAAGGCC
MET15-F	GTTTAAGGCGTCAGATTTAGGTGG
MET15-R	TTGCTGATTATGTACTCAGTTTAACG

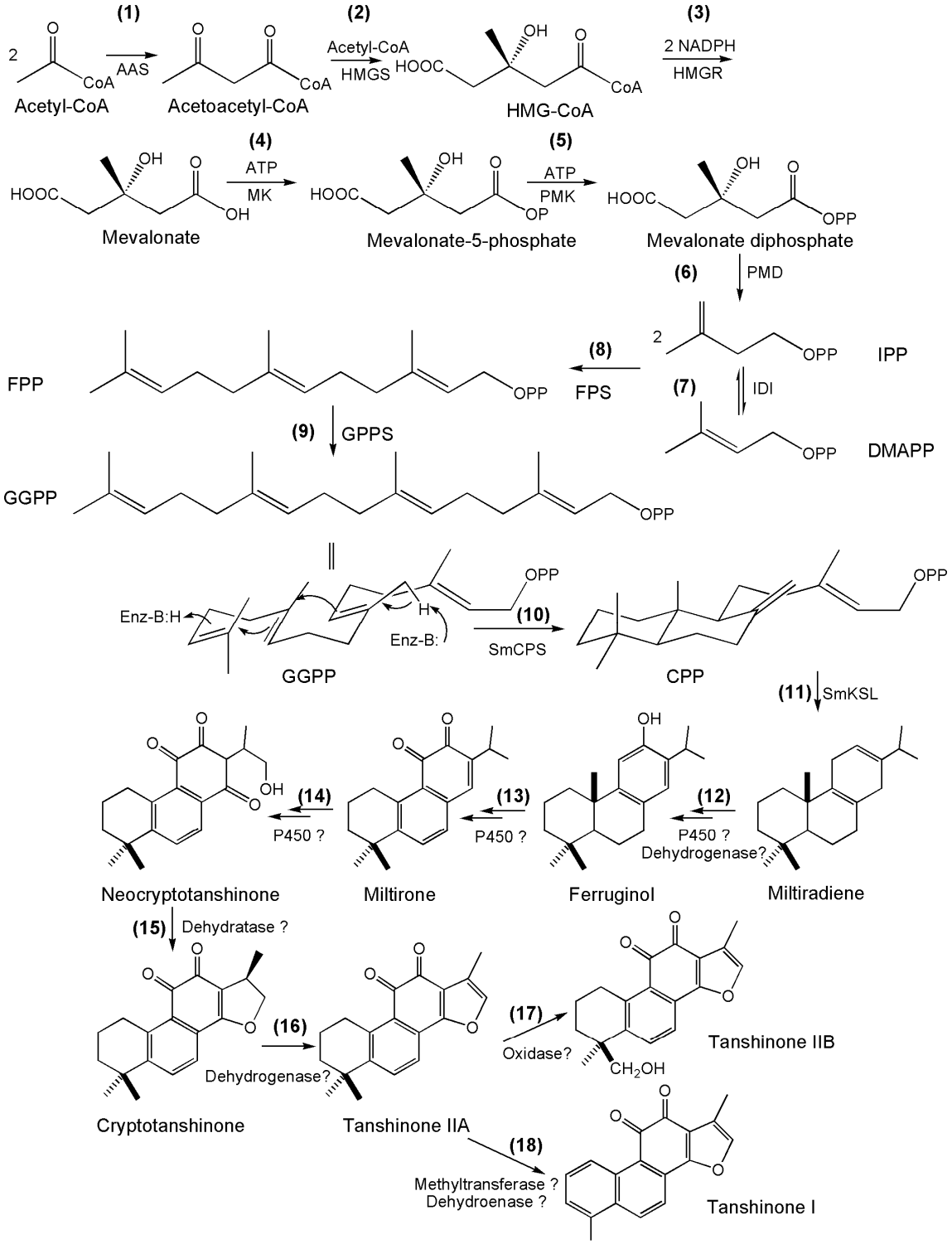

Figure S1. Hypothetical tanshinone biosynthetic pathway. The miltiradiene is synthesized from GGPP by copalyl diphosphate synthases (SmCPS) and kaurene synthase-like (SmKSL), and then is transformed to different tanshinones catalyzed by series of P450 and other enzymes.

a)

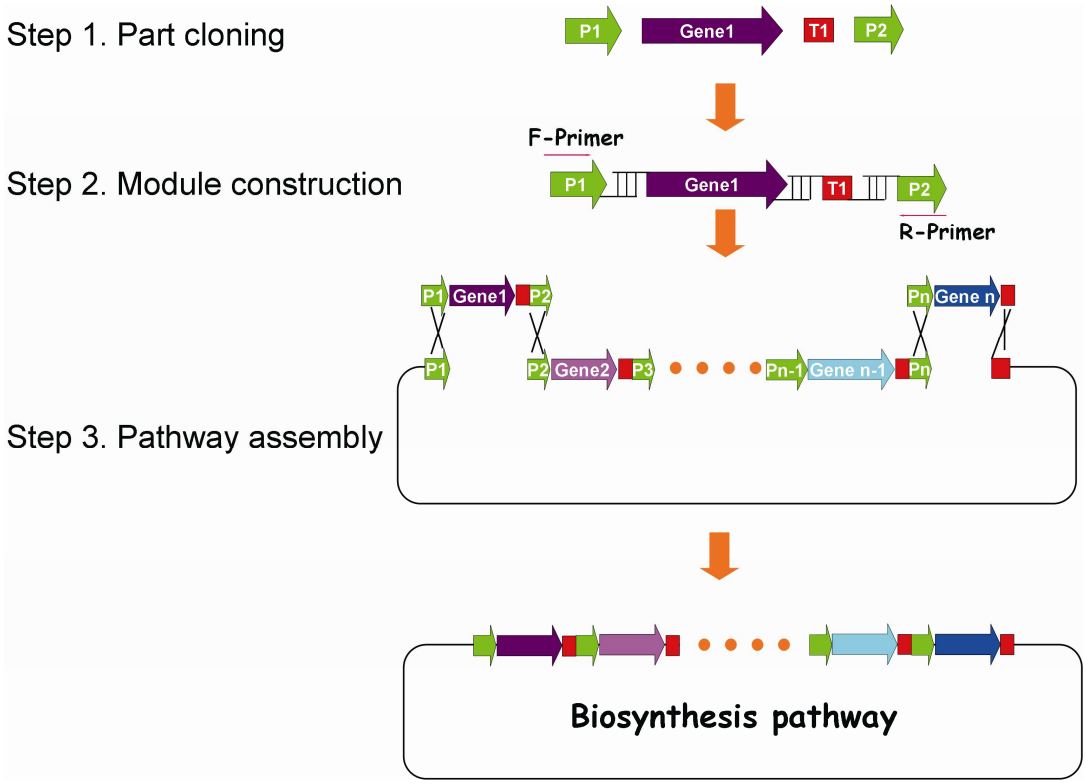

b)

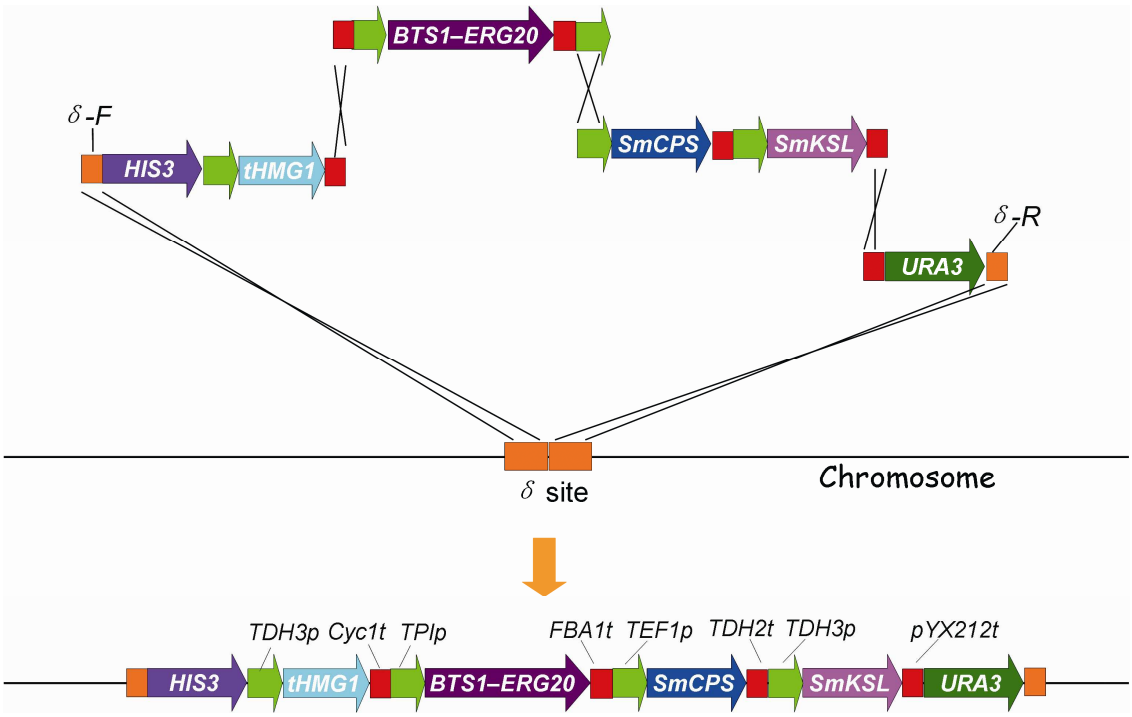

Figure S2. Schematic illustration of the modular pathway engineering strategy for rapid pathway construction. (a) Biosynthetic pathway construction on episomal plasmid pYX212. Parts (including promoter, functional genes, terminators, etc) were cloned at step1; Modules was constructed by one-step SOE PCR amplification using parts prepared at Step1. To ensure

individual module functioning, each gene is linked with a promoter and a terminator. Moreover, homologous sequences (~ 400 bp) overlapping with adjacent modules are introduced at the 5'- and 3'-termini to mediate *in vivo* homologous recombination in the Pathway assembly step. To construct each module according to splice over-lap extension (SOE) PCR in a part-by-part way would be laborious and time consuming, because an expression module consisting of three parts and homologous sequences required at least two consecutive SOE PCR procedures. We found, by carefully tuning the molecular ratios among parts and the PCR condition described in the DNA Manipulation of Experimental Procedures section, an expression module could be realized with one-step SOE PCR. We successfully constructed all modules contained up to 4 parts and up to 6.5 kb in DNA length with the one-step SOE PCR procedure. Therefore, a functional module could be produced within 10 h once the cloning experiments were started for the corresponding parts. In this work, the expression vector pYX212 was used in the Pathway assembly step, such that the first and the last module of the designed pathway should have homologous sequences overlapping with those on the vector. The expression modules were co-transformed by electroporation with linearized vector pYX212 into *S. cerevisiae* BY4741, and the recombinants appeared on the corresponding plates after 2–4 days. We constructed 7 pathways in 1 week with an overall positive rate of 88%. (b) The optimized miltiradiene biosynthetic pathway was assembled and integrated into δ sites of chromosome with modular pathway engineering strategy. we constructed four modules: module A (δ1-*HIS3-TDH3*p-*tHMG1-CYC1*t) consisted of the upper regions of δ integration site, *HIS3* marker and *tHMG1*; module B (*CYC1*t-*TPI*p-(*BTS1-ERG20*)-*FBA1*t-*TEF1*p), consisted of the *BTS1-ERG20* gene; module C (*TEF1*p-*SmCPS-TDH2t-TDH3p-SmKSL-pYX212t*) consisted of *SmCPS* and *SmKSL*; module D (*pYX212t-URA3*-δ2) consisted of the selection marker *URA3* and the downstream region of δ integration site. The integration experiment was done by co-transforming the 4 modules into *S. cerevisiae* BY4741, leading to the a-type miltiradiene-producing strain YJ21.

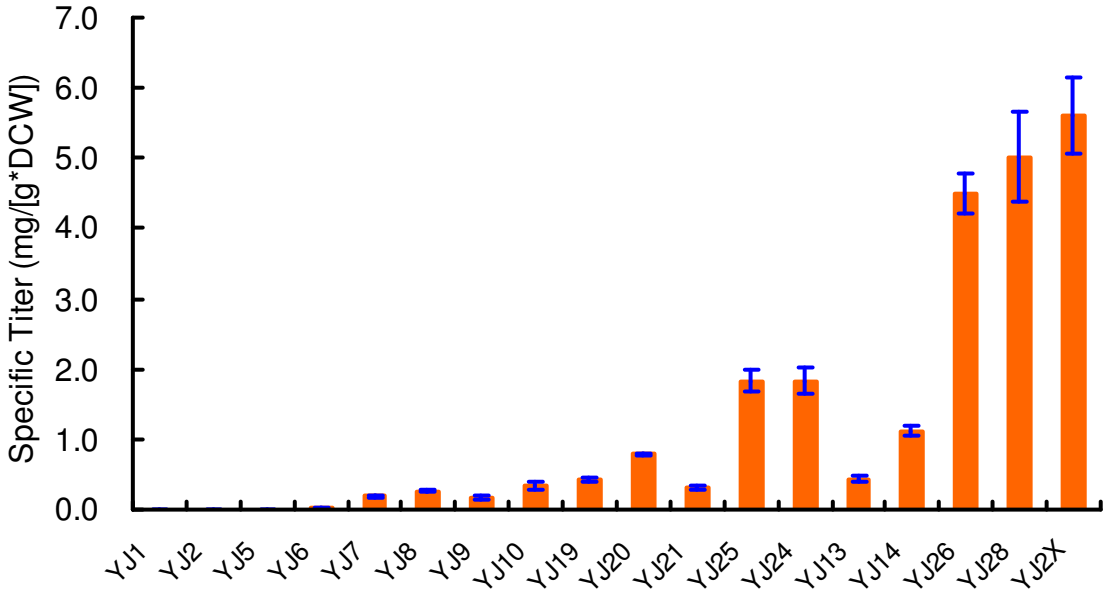

Figure S3. The specific miltiradiene titer in recombinant *S. cerevisiae* strains. Miltiradiene were extract with hexane from the strains after 48 h cultivation in YPD medium. The cell dry weight was calculated from a calibration curve relating OD600 to dry weight with a factor of one OD_{600} = 0.266 mg dry cell/ml.[1]

a)

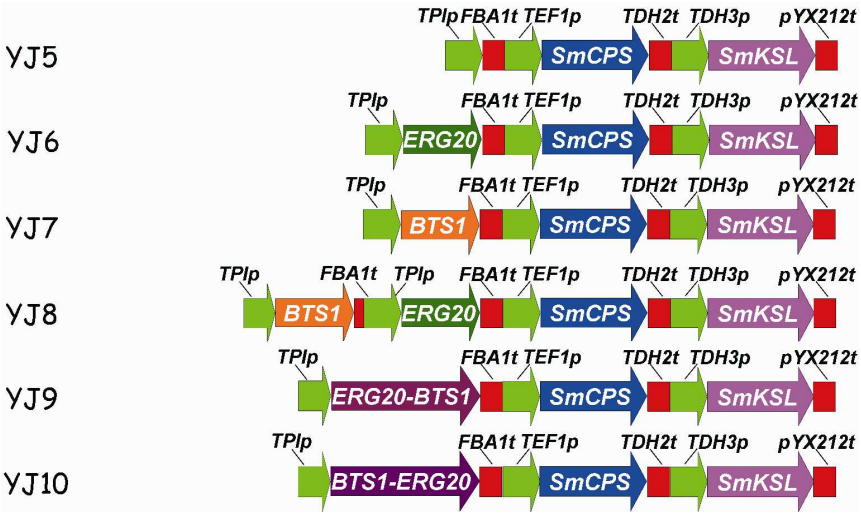

b)

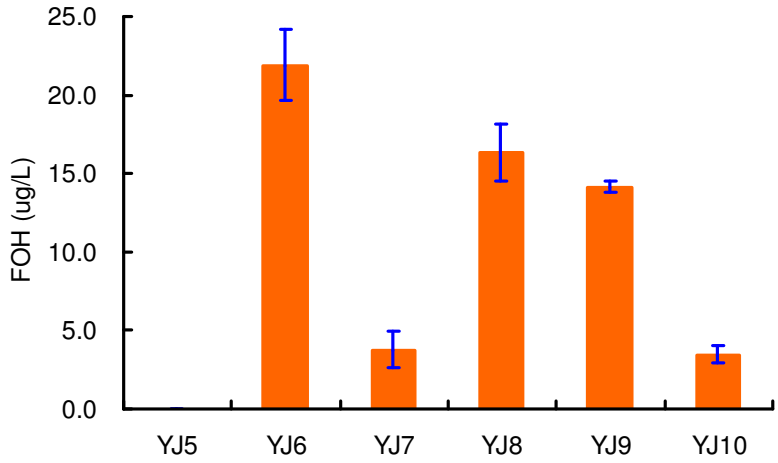

Figure S4. BTS1-ERG20 fusion decreased FOH level. (a) The schematic representation of biosynthetic pathways containing BTS1-ERG20 fusion enzyme for miltiradiene production. (b) The FOH increased to 21.9 μg/L in ERG20 overexpressing strain and decreased to 3.7 μg/L when BTS1 overexpressed. Strain YJ10 containing BTS1-ERG20 pathway has much lower FOH accumulation (3.4 μg/L) compared with strain YJ9 containing ERG20-BTS1 fusion pathway (14.1 μg/L), which was negative correlation with miltiradiene yield.

a)

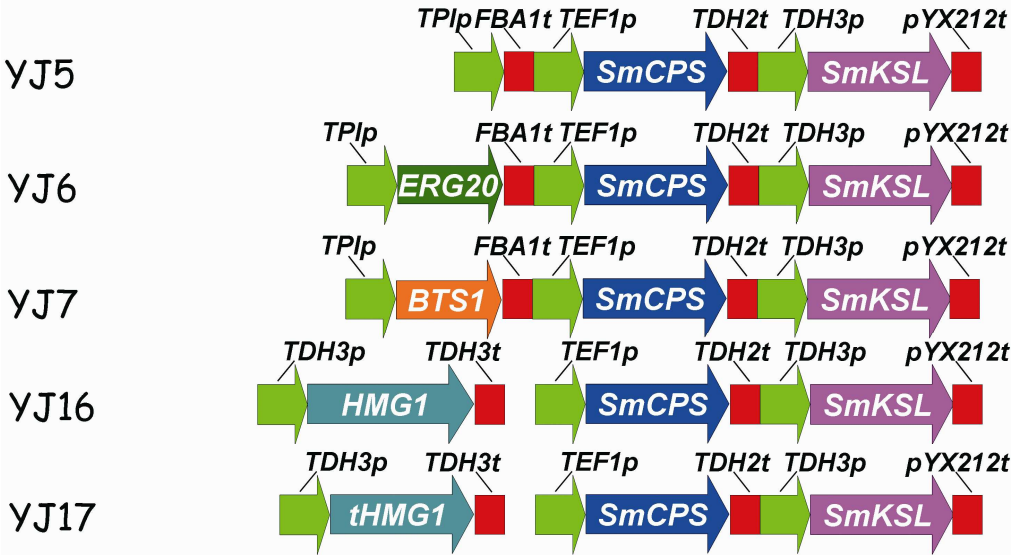

b)

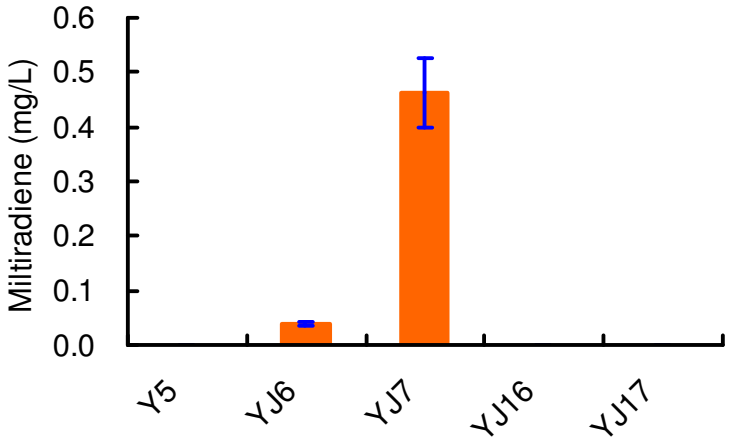

Figure S5. The BTS1 not the tHMG1 was the key enzyme for miltiradiene production.

(a) The schematic representation of biosynthetic pathways for miltiradiene production. (b) Miltiradiene production by recombinant strains overexpressing *ERG20*, *BTS1*, *HMG1 and tHMG1* genes with episomal plasmids in flask shake cultures. Over-expressing the HMG-CoA reductase gene *HMG1* and its catalytic domain *tHMG1* had no miltiradiene production, and *ERG20* overexpression increased little miltiradiene yield. However, *BTS1* overexpression increased the miltiradiene biosynthesis significantly to 0.5 mg/L. The data represent the averages ± standard deviations of three independent clones.

a)

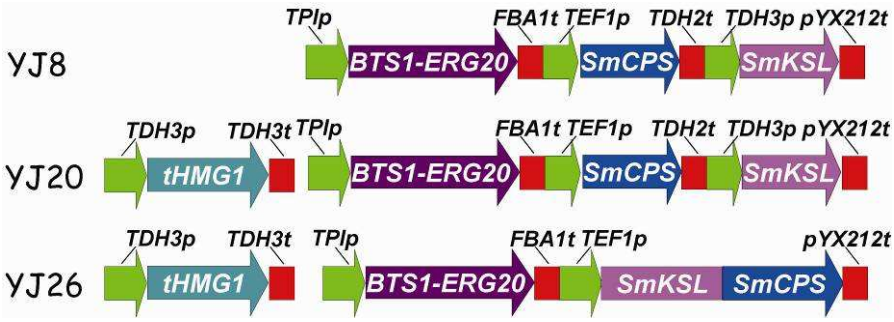

b)

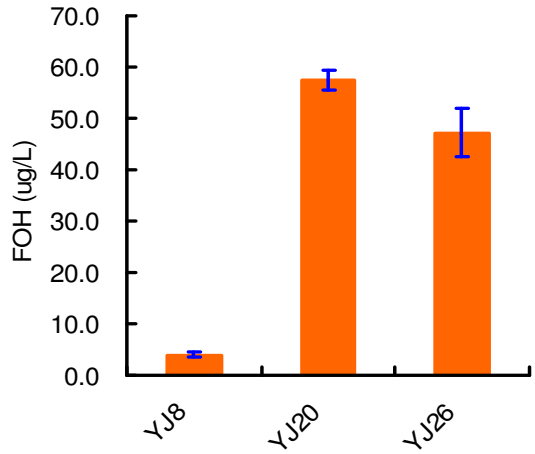

c)

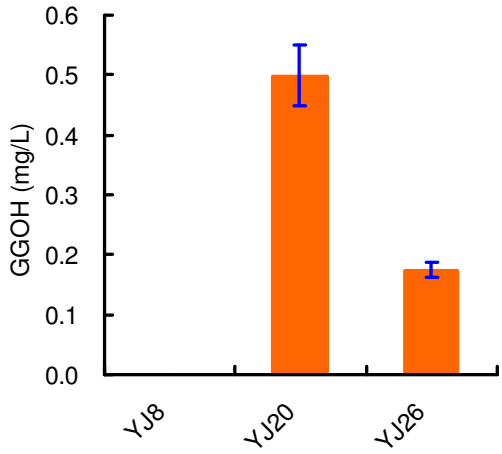

Figure S6. SmKSL-SmCPS fusion decreased FOH and GGOH levels.

(a) The schematic representation of miltiradiene biosynthetic pathways in *S. cerevisiae*. (b) The FOH accumulation increased to 57.4 μg/L in YJ20 containing an enhanced MVA pathway due to *tHMG1* overexpression, and had a slight decrease in YJ26 (47.2 μg/L) containing SmKSL-SmCPS fusion pathway. (c) GGOH accumulation in YJ20 reached to 0.53 mg/L and decreased significantly in YJ26 (0.17 mg/L), which demonstrated the SmKSL-SmCPS fusion could converse GGPP to miltiradiene with higher efficiency than separate enzymes.

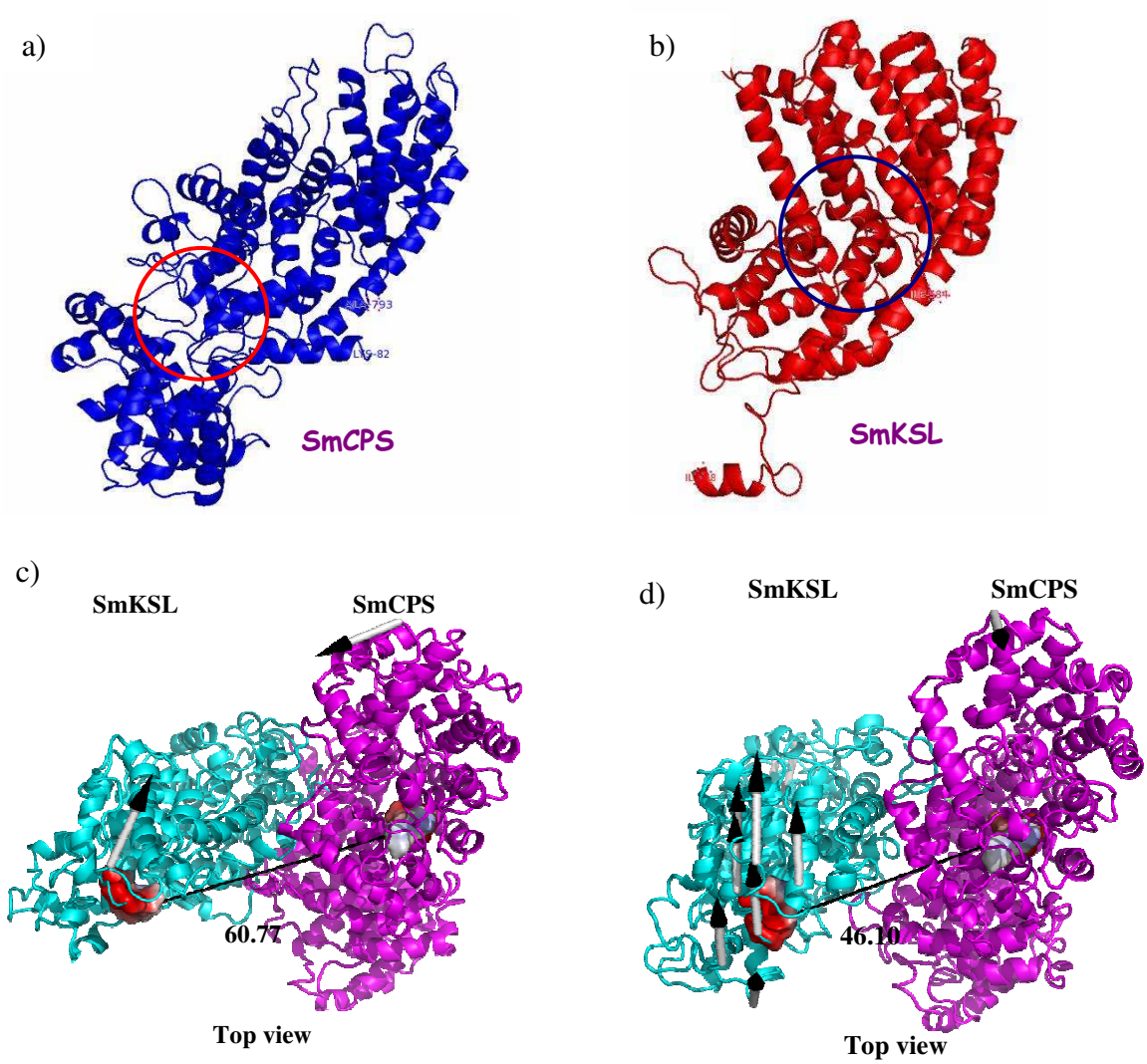

Figure S7. The modeling structure of SmCPS and SmKSP.

(a) Protein modeling of SmCPS in Swiss-model[2] using AtCPS as a template[3] (48% identity) showed it was belong to class II synthase containing α, β and γ domains and the active site DXDD motif for H^+-initiated cyclization is located between the β and γ domains in the N-terminal (red cycle). (b) Protein modeling of SmKSL in Swiss-model using TbTS[4] as a template showed they are belong to class I synthase containing α and β domains and the active site DDXXD motif for proton-initiated cyclization in α domain (blue cycle). (c) The top view the modeling structure of SmCPS-SmKSL. (d) The top view the modeling structure of SmKSL-SmCPS.

Because SmCPS had additional 89 amino acids at the N-terminal compared to the crystal structure of AtCPS (PDB code 3PYB), these N-terminal sequence in SmCPS were built using glutathione S-transferase (PDB code 1GWC)[5] as the template (sequence identity 24%).

Sequences were imported into the ClustalW program for the alignment,[6] and ORCHESTRAR module in SYBYLx1.1 (Tripos Associates, St. Louis) was used to build the initial three-dimensional structure of SmCPS and SmKSL.

Since the two fusion protein complexes (SmCPS-SmKSL and SmKSL-SmCPS) are unknown, the initial 15 conformations for each complex were constructed by manually changing the relative positions of SmCPS and SmKSL linked by GGGS. Since the fusion protein complex (1392 residues) is too large to run full atomistic molecular dynamics (MD) simulation with explicit solvent model, the simulation was carried out by utilizing the simplest implicit solvent model, which is distance-dependent dielectric constant, to mimic solvent effect on protein conformations. Energy minimization and MD simulations were performed using the sander module of Amber 10.0[7] to obtain the most stable and predominant fusion structures of SmCPS and SmKSL. Energy minimization was performed using the steepest descent minimization of 5000 steps followed by 5000-step conjugate gradient minimization. The SHAKE algorithm was applied to constrain all bonds involving hydrogen. The particle mesh ewald method was adopted to treat long range electrostatic interactions. The time step of all molecular dynamics simulations was 2 fs, and the non-bonded cutoff was 10 Å. MD simulations were performed on each system up to 10ns. To monitor the stability of each MD simulation, the root-mean-squared deviation (RMSD) was calculated utilizing the ptraj module in Amber 10.0 and the distance between active sites of SmCPS and SmKSL were also measured. The averaged structure for each simulation was made with 1000 snapshots collected over last 2 ns simulation, and it was further refined by following short-time MD simulations with more realistic implicit solvent model, which is Generalized-Born (GB) implicit solvent model. For each fusion protein, the structure with lowest potential energy including GB solvation energy among all the refined models was selected as the target for further dynamics investigation by normal mode analysis (NMA).

Biological phenomena usually relate to large-scale protein motions, which associate with the low frequency normal modes, especially the lowest one. The most predominant structures derived from above analysis were subject to normal mode analysis to get more insights about

the dynamics of the system. The normal mode analysis was performed by the ANM server (http://ignmtest.ccbb.pitt.edu/cgi-bin/anm/anm1.cgi).[8, 9]

a)

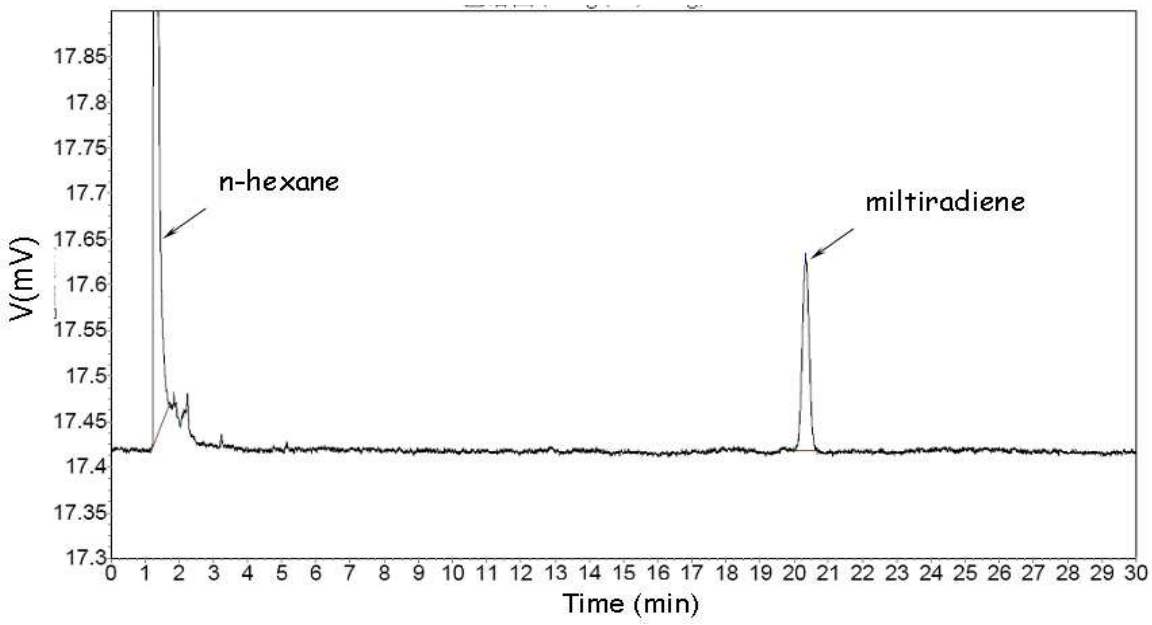

b)

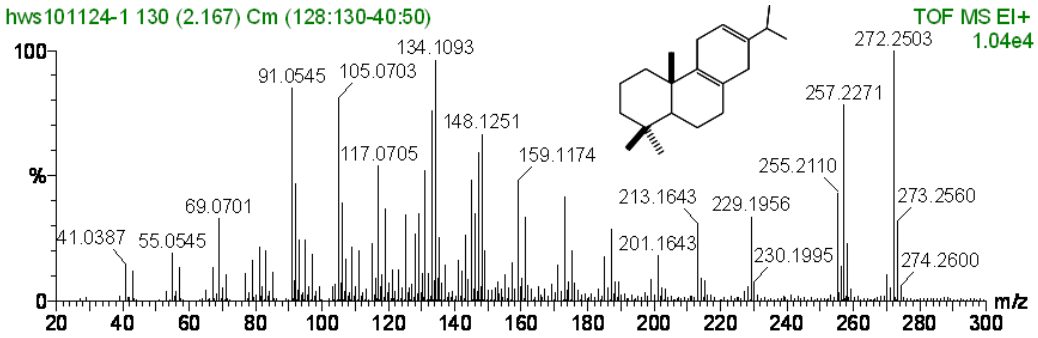

Figure S8. GC-MS of purified miltiradiene from the engineered yeast strain. Because miltiradiene is not commercially available, so we extracted and purified the miltiradiene for quantitative analysis. (a) Gas chromatogram of the miltiradiene (retention time 20.34 min). (b) High resolution mass spectrometry of the miltiradiene (MW = 272.2503).

a)

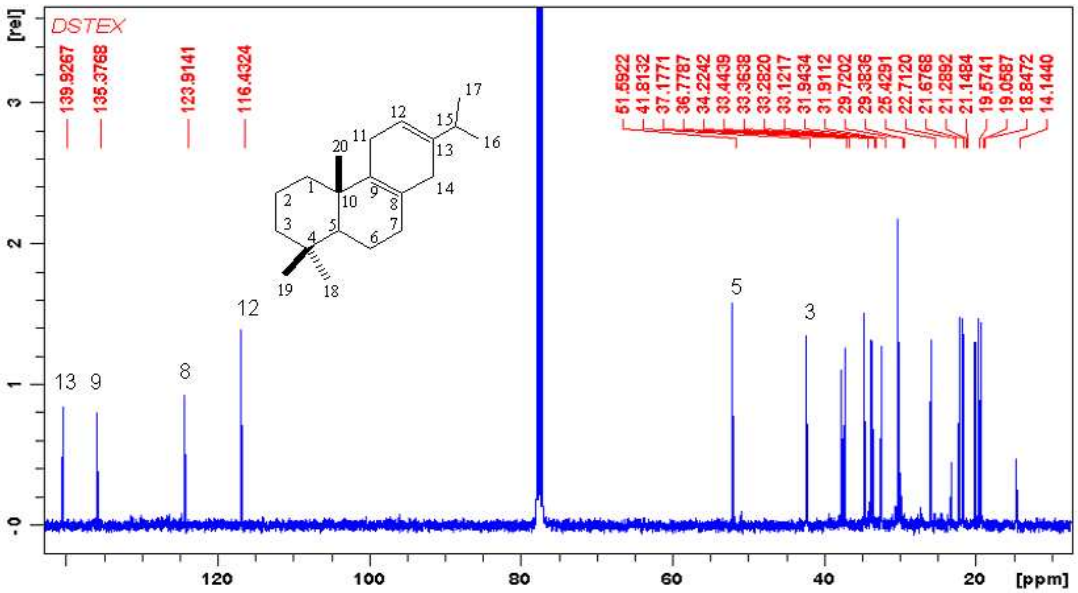

b)

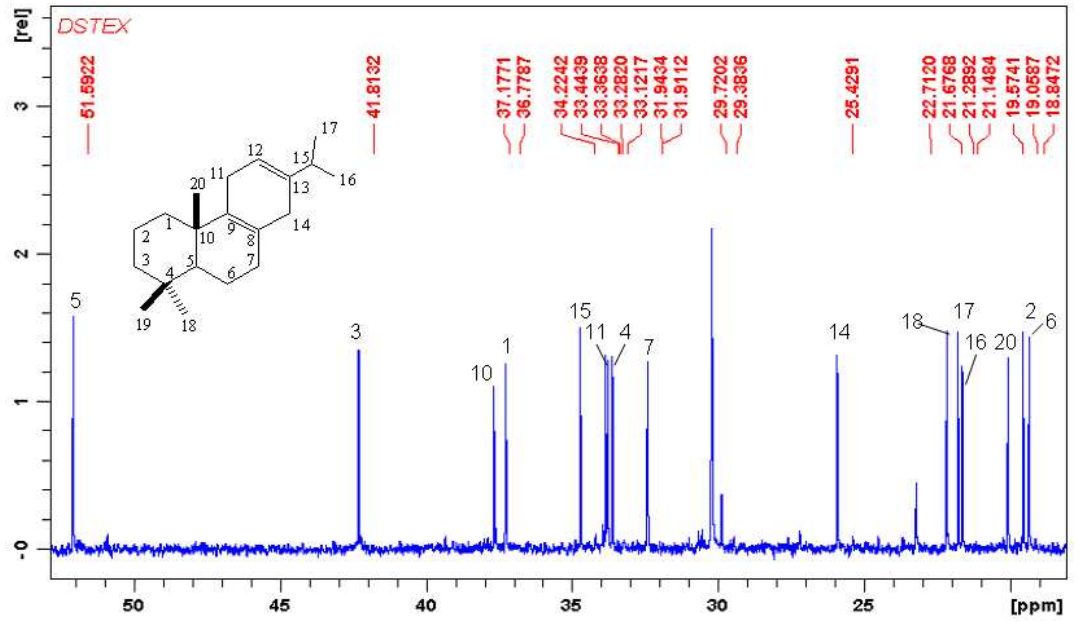

Figure S9. ^{13}C-NMR spectra of miltiradiene. Experiment was recorded in chloroform-d at 25 °C on a Bruker DRX 400 equipped with a probe with cryogenic detection. Structural analysis was performed using the Bruker TopSpin software. Chemical shifts were referenced to the known chloroform-d signals offset from TMS. (a) Full spectra. (b) Detailed upfield spectra.

a)

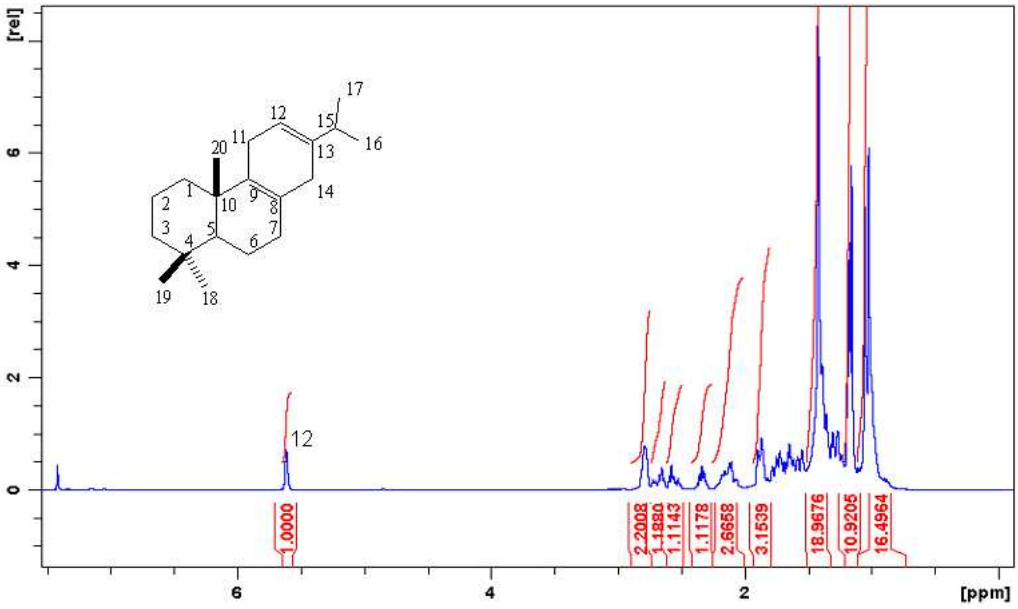

b)

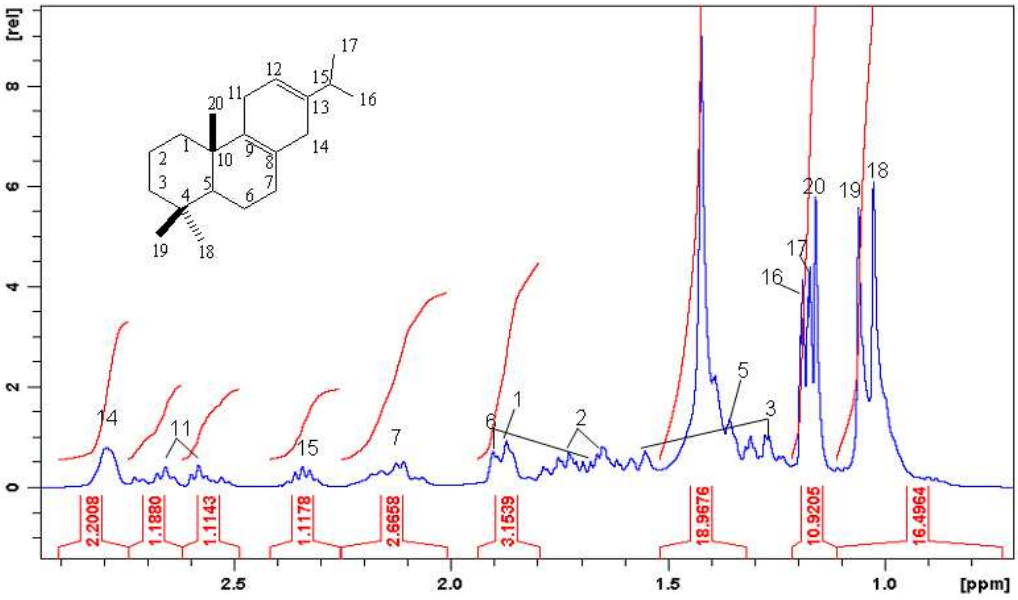

Figure S10. ^{1}H-NMR spectra of miltiradiene. Experiment was recorded in chloroform-d at 25 °C on a Bruker DRX 400 equipped with a probe with cryogenic detection. Structural analysis was performed using the Bruker TopSpin software. Chemical shifts were referenced to the known chloroform-d signals offset from TMS. (a) Full spectra. (b) Detailed upfield spectra.

References:

1. Lee, F.J.S.; Hassan, H.M. *Appl. Microbiol. Biotechnol.* **1987**, *26*, 531–536.
2. Bordoli, L.; Kiefer, F.; Arnold, K.; Benkert, P.; Battey, J.; Schwede, T. *Nat. Protoc.* **2009**, *4*, 1–13.
3. Koksal, M.; Hu, H.; Coates, R. M.; Peters, R. J.; Christianson, D. W. *Nat. Chem. Biol.* **2011**, *7*, 431–433.
4. Koksal, M.; Jin, Y.; Coates, R. M.; Croteau, R.; Christianson, D. W. *Nature* **2011**, *469*, 116–120.
5. Thom, R.; Cummins, I.; Dixon, D. P.; Edwards, R.; Cole, D. J.; Lapthorn, A. J. *Biochemistry* **2002**, *41*, 7008–7020.
6. Thompson, J. D.; Higgins, D. G.; Gibson, T. J. *Nucleic Acids Res.* **1994**, *22*, 4673–4680.
7. Case, D. A. et al. *AMBER 10*, University of California, San Francisco (**2008**).
8. Atilgan, A. R.; Durell, S. R.; Jernigan, R. L.; Demirel, M. C.; Keskin, O.; Bahar, I. *Biophys. J.* **2001**, *80*, 505–515.
9. Bakan, A.; Bahar, I. *Proc. Natl. Acad. Sci. USA* **2009**, *106*, 14349–14354.